Suppporting Information

Remarkable direct formic acid electrocatalysis enabled by rare earth-doped platinum-tellurium heterostructures

Xin Lin[1], Shize Geng[1], Xianglong Du[2], Feiteng Wang[2], Xu Zhang[1], Fang Xiao[1], Zhengyi Xiao[2], Yucheng Wang[2], Jun Cheng[2], Zhifeng Zheng[1], Xiaoqing Huang[2] & Lingzheng Bu[1*]

[1]College of Energy, Xiamen University, Xiamen, 361102, P. R. China.

[2]State Key Laboratory of Physical Chemistry of Solid Surfaces, College of Chemistry and Chemical Engineering, Xiamen University, Xiamen, 361005, P. R. China.

[*]To whom correspondence should be addressed.

E-mail: lzbu@xmu.edu.cn

Supplementary Figures and Tables:

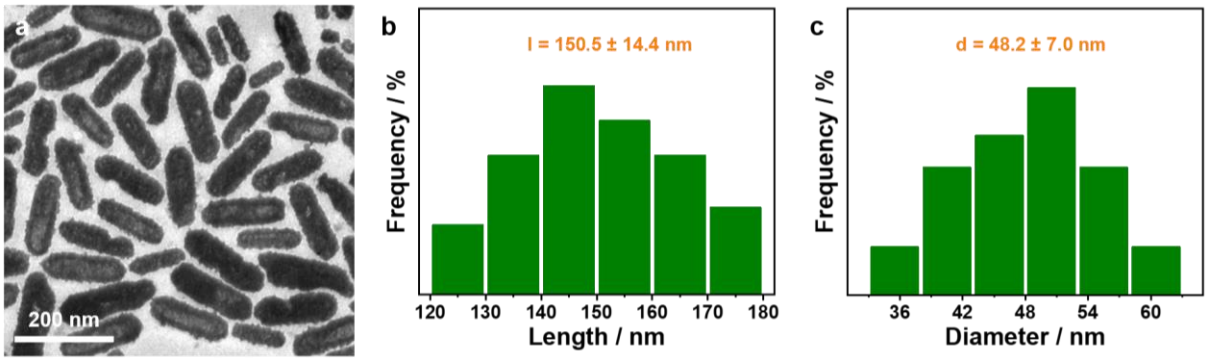

Supplementary Figure 1. (a) TEM image, (b) length distribution and (c) diameter distribution of (Y-Pt)-$PtTe_2$ HPNT.

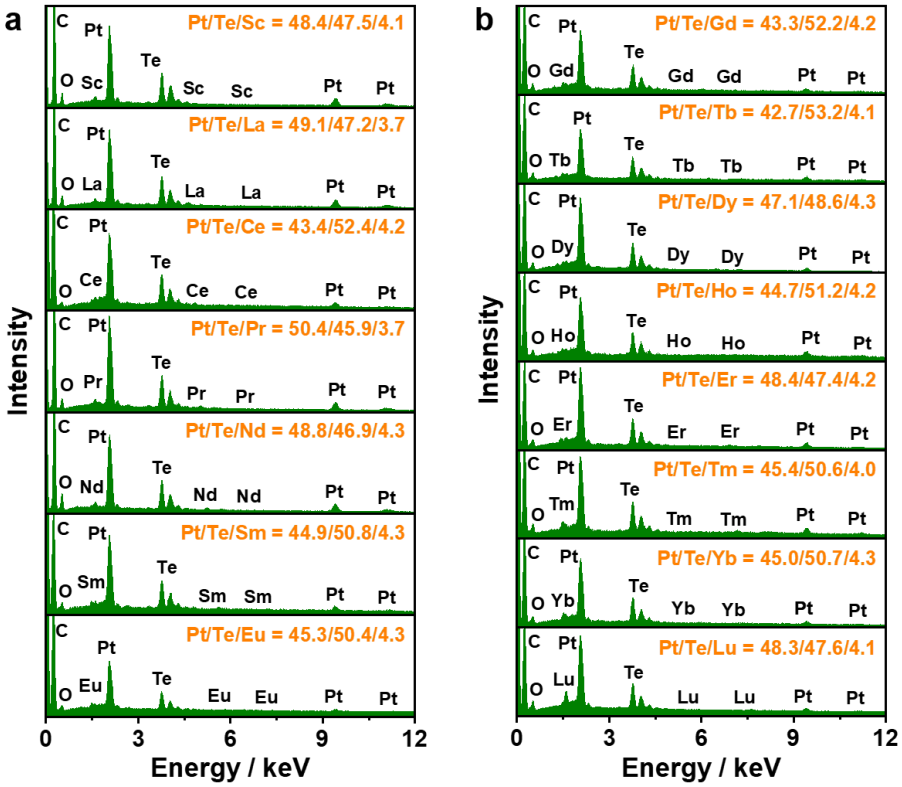

Supplementary Figure 2. SEM-EDS of other (RE-Pt)-$PtTe_2$ HPNT, where RE represent (a) Sc, LREE and (b) HREE (except for Y) metals.

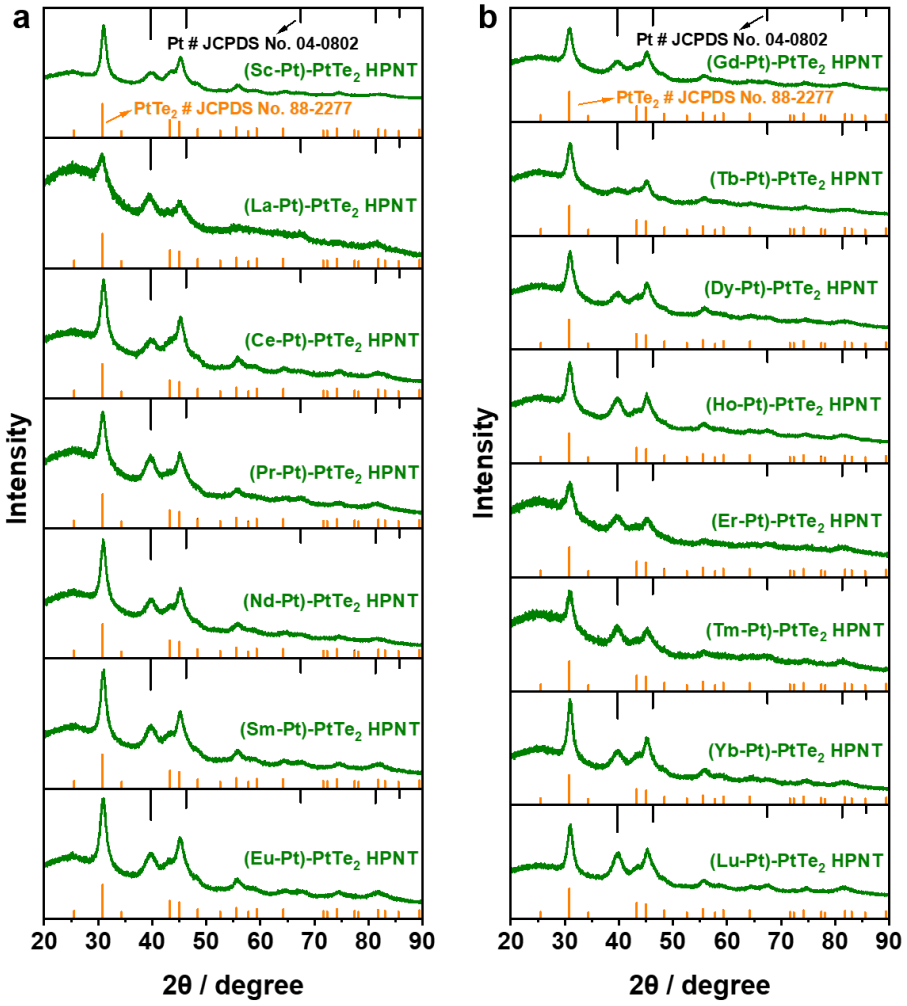

Supplementary Figure 3. XRD patterns of other (RE-Pt)-$PtTe_2$ HPNT, where RE represent (a) Sc, LREE and (b) HREE (except for Y) metals.

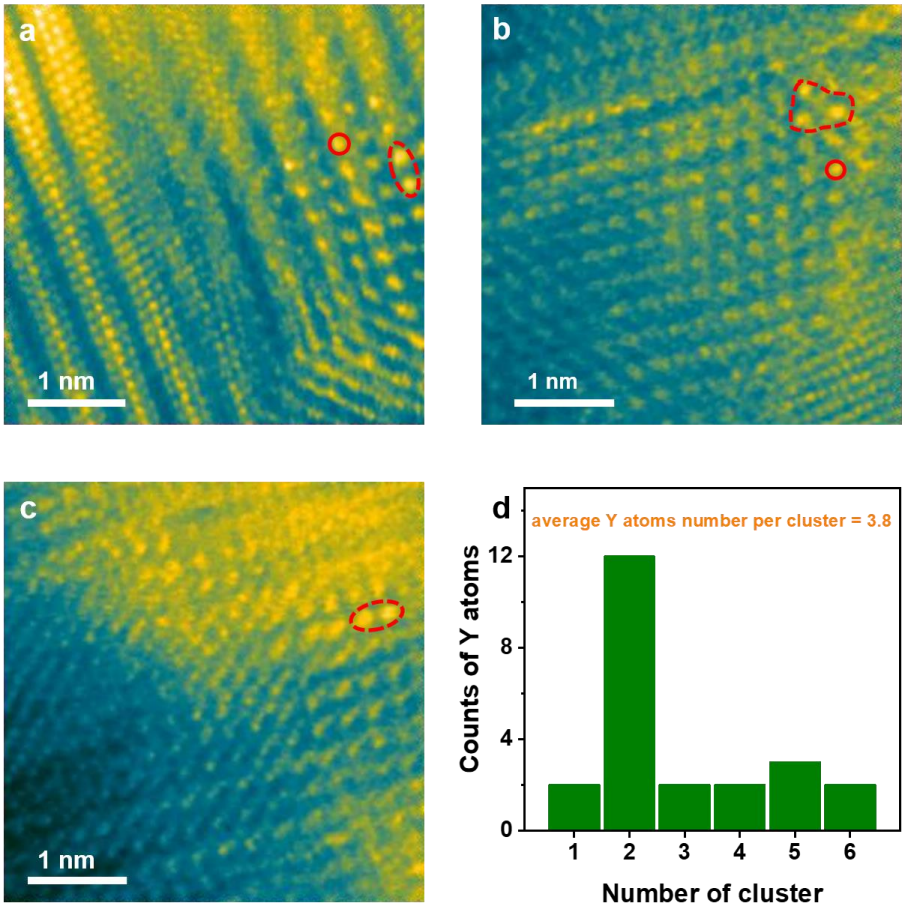

Supplementary Figure 4. (a-c) Additional AC-HAADF-STEM images of (Y-Pt)-$PtTe_2$ HPNT. (d) Statistics of Y atoms number for clusters in (Y-Pt)-$PtTe_2$ HPNT.

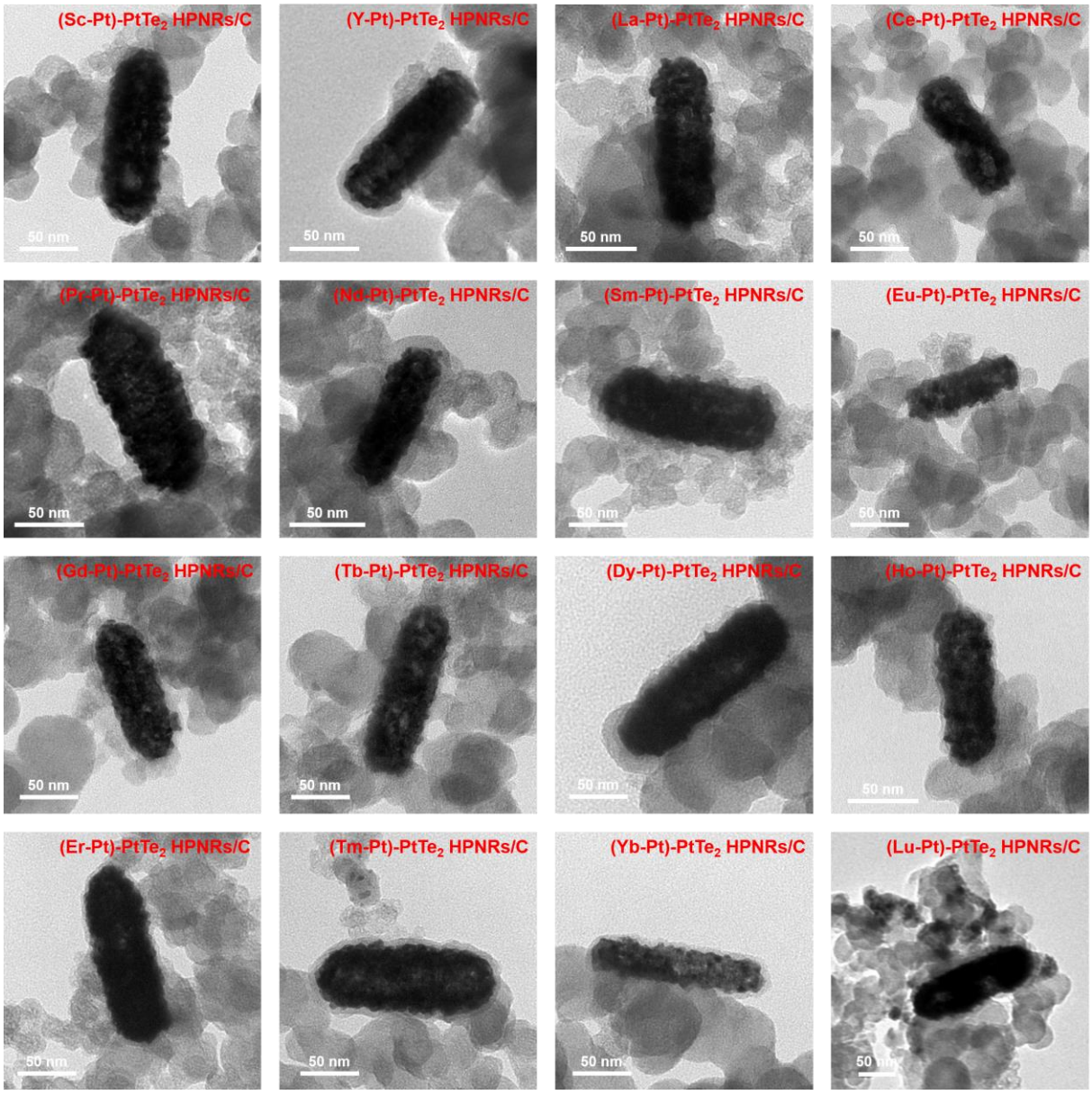

Supplementary Figure 5. TEM images of all (RE-Pt)-$PtTe_2$ HPNT/C, where RE represent all RE metals except for Pm.

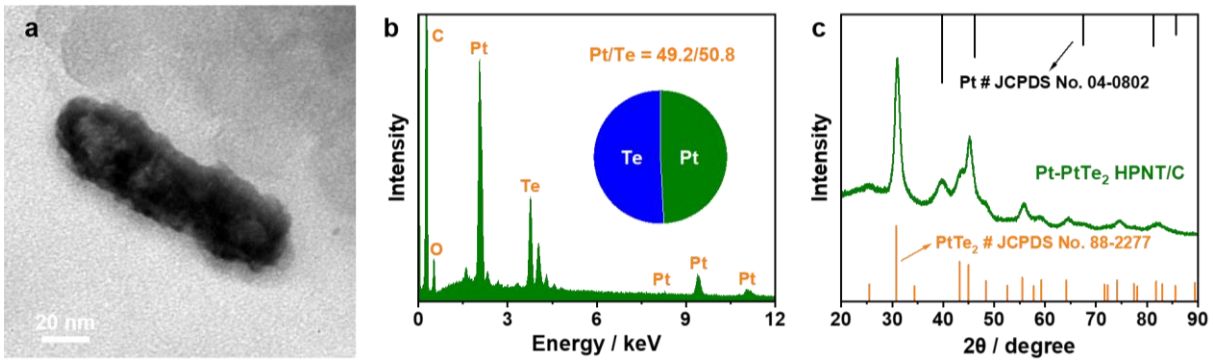

Supplementary Figure 6. (a) TEM image, (b) SEM-EDS and (c) XRD pattern of Pt-$PtTe_2$ HPNT/C.

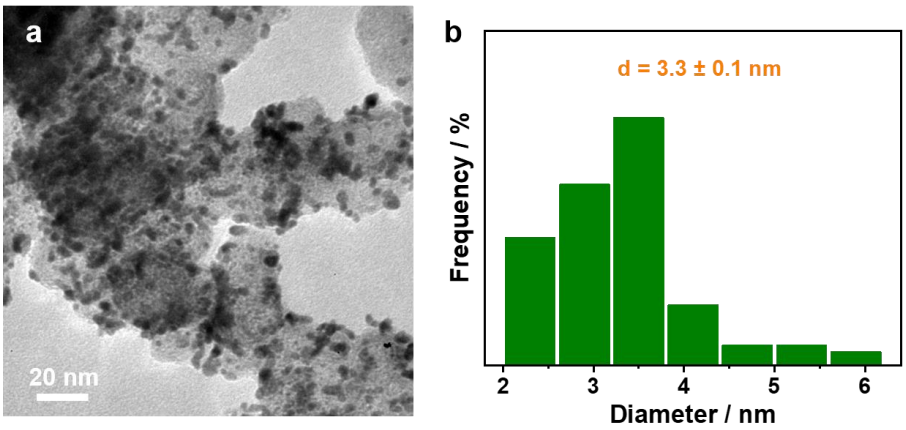

Supplementary Figure 7. (a) TEM image and (b) diameter distribution of commercial Pt/C.

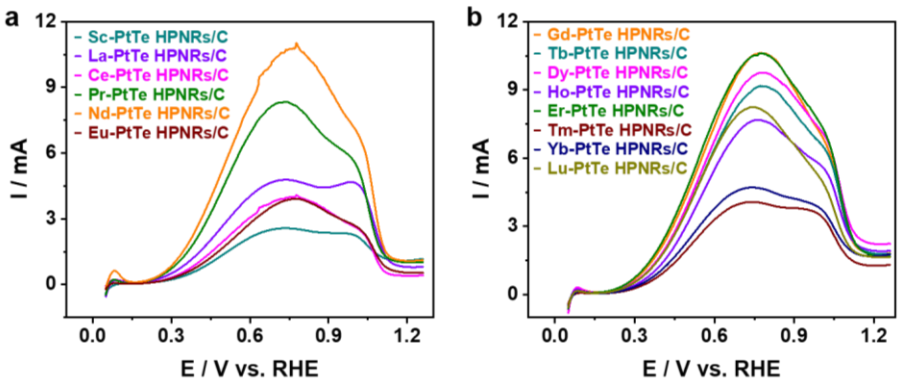

Supplementary Figure 8. Forward-scan CV curves of other (RE-Pt)-$PtTe_2$ HPNT/C catalysts toward FAOR, where RE represent (a) Sc, LREE (except for Sm) and (b) HREE (except for Y) metals.

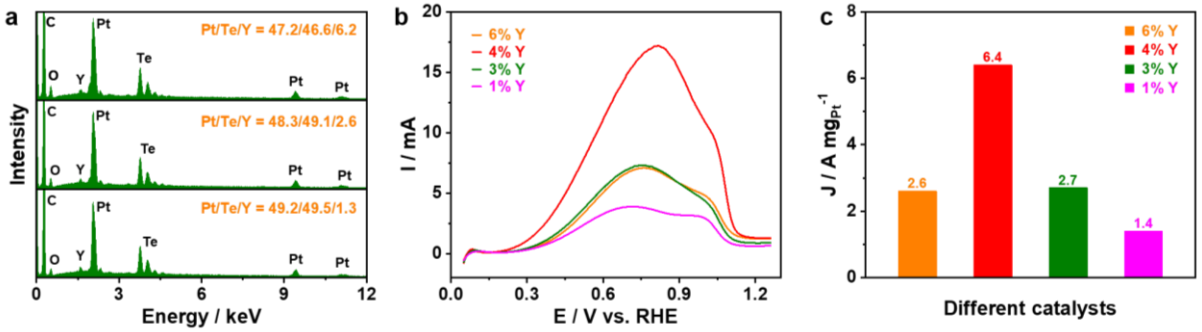

Supplementary Figure 9. (a) SEM-EDS, (b) CV curves and (c) mass activities of (Y-Pt)-$PtTe_2$ HPNT/C with different Y doping amounts (1%, 3%, 4% and 6%).

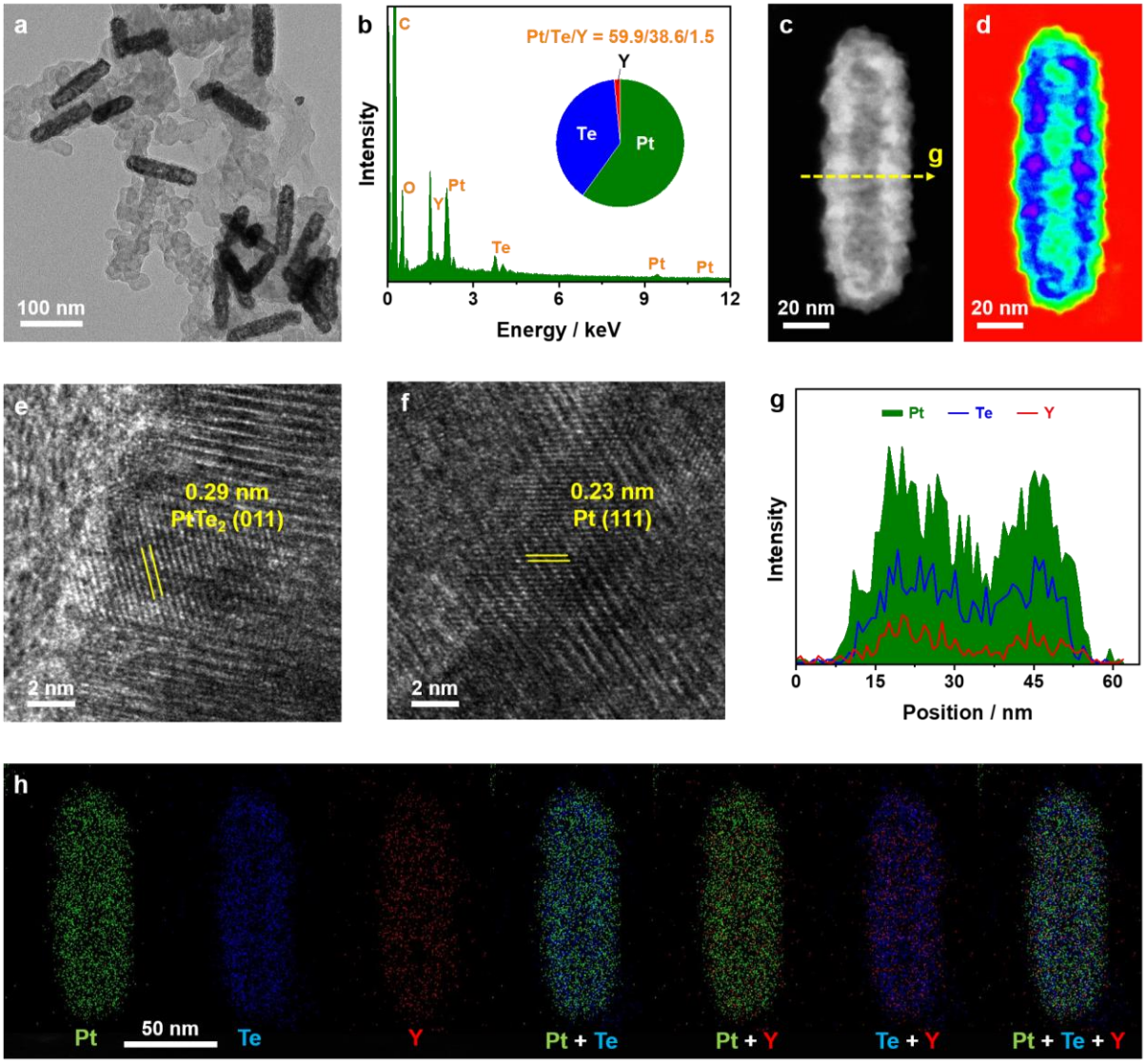

Supplementary Figure 10. (a) TEM image, (b) SEM-EDS, (c, d) HAADF-STEM and corresponding rainbow-colored images, (e, f) HRTEM images, (g) line scan, and (h) corresponding elemental mappings of (Y-Pt)-$PtTe_2$ HPNT/C after the chronoamperometry test.

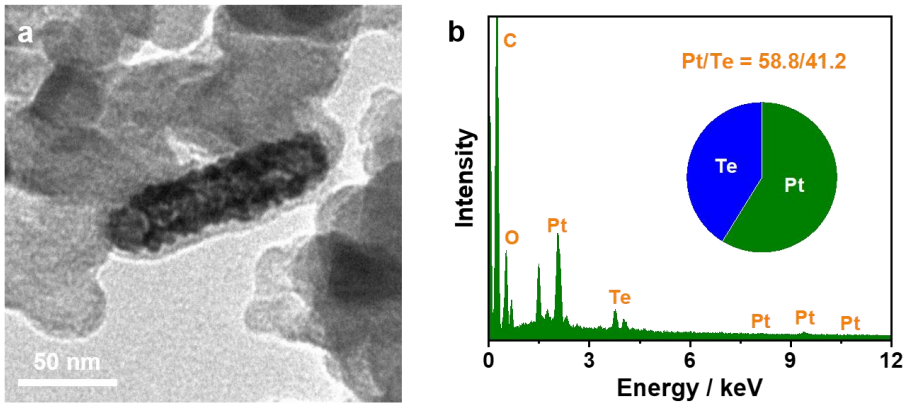

Supplementary Figure 11. (a) TEM image and (b) SEM-EDS of Pt-$PtTe_2$ HPNT/C after the chronoamperometry test.

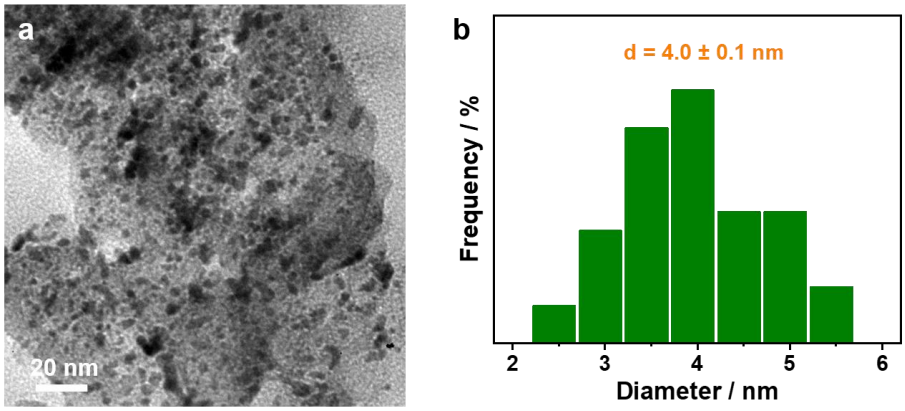

Supplementary Figure 12. (a) TEM image and (b) diameter distribution of commercial Pt/C after the chronoamperometry test.

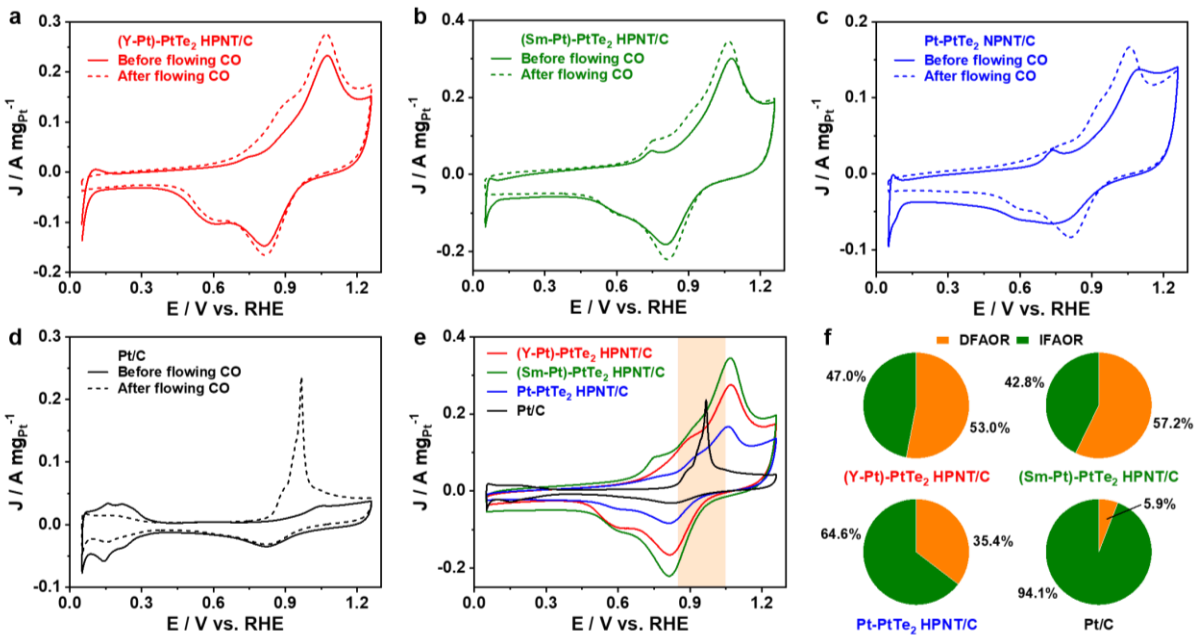

Supplementary Figure 13. CO stripping curves of (a) (Y-Pt)-$PtTe_2$ HPNT/C, (b) (Sm-Pt)-$PtTe_2$ HPNT/C, (c) Pt-$PtTe_2$ HPNT/C and (d) commercial Pt/C in CO-injected 0.5 M H_2SO_4. (e) Comparison of CV curves for different catalysts after flowing CO into 0.5 M H_2SO_4. (f) Reaction tendency of different catalysts after flowing CO into 0.5 M H_2SO_4 + 0.5 M HCOOH.

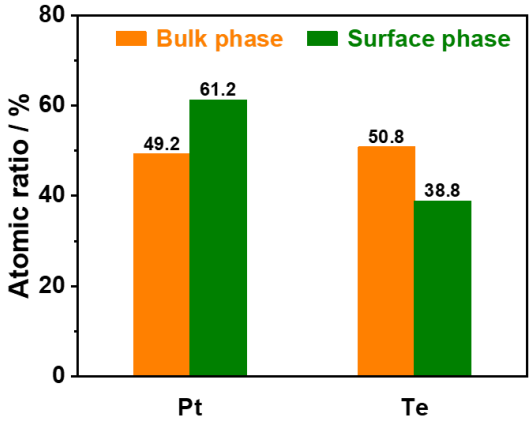

Supplementary Figure 14. Atomic ratios of Pt and Te in the bulk phase and surface phase of Pt-$PtTe_2$ HPNT/C.

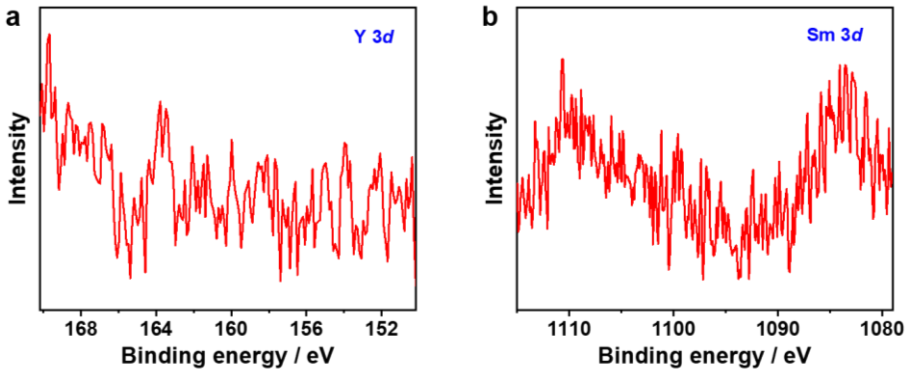

Supplementary Figure 15. (a) Y 3*d* XPS spectrum of (Y-Pt)-$PtTe_2$ HPNT/C. (b) Sm 3*d* XPS spectrum of (Sm-Pt)-$PtTe_2$ HPNT/C.

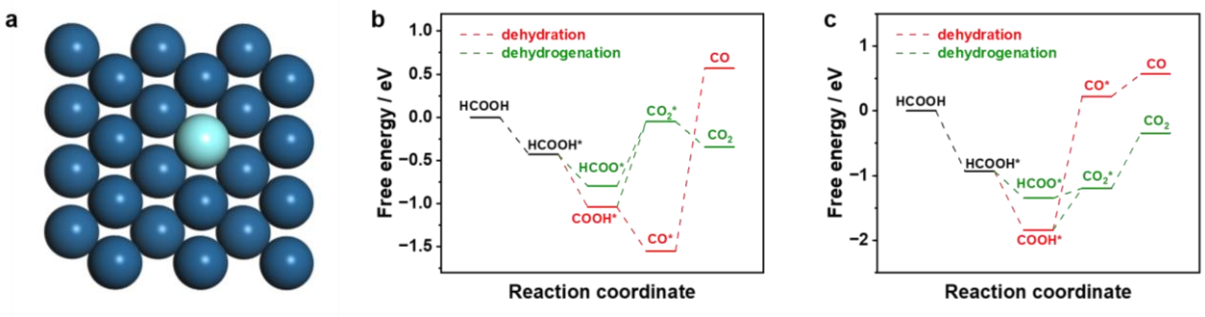

Supplementary Figure 16. (a) Slab model of Pt (110) surface with single Y site. The corresponding reaction energy diagrams of (b) Pt adsorption site and (c) Y adsorption site.

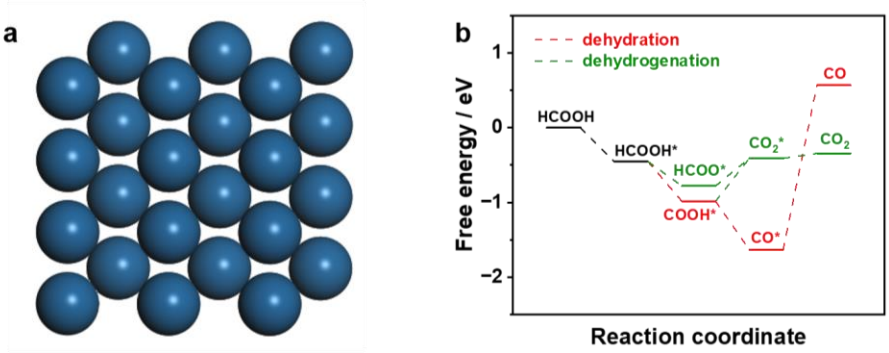

Supplementary Figure 17. (a) Slab model of Pt (110) surface. (b) The corresponding reaction energy diagram of Pt adsorption site.

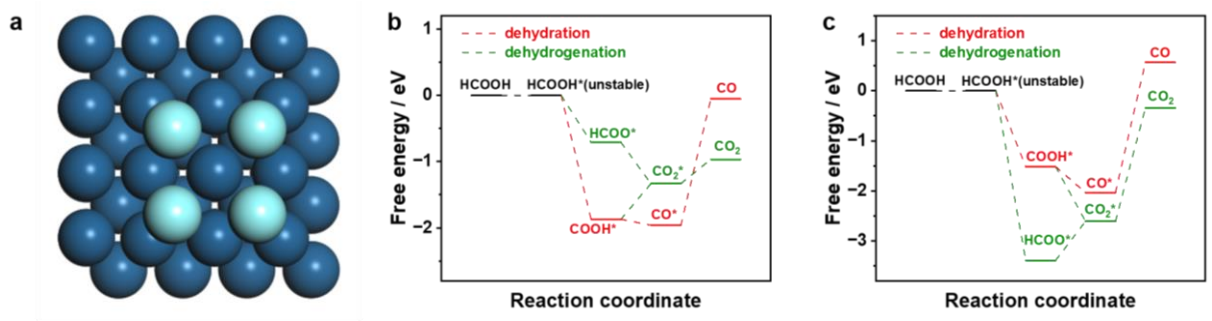

Supplementary Figure 18. (a) Slab model of Pt (100) surface with Y cluster. The corresponding reaction energy diagrams of (b) Pt adsorption site and (c) Y adsorption site.

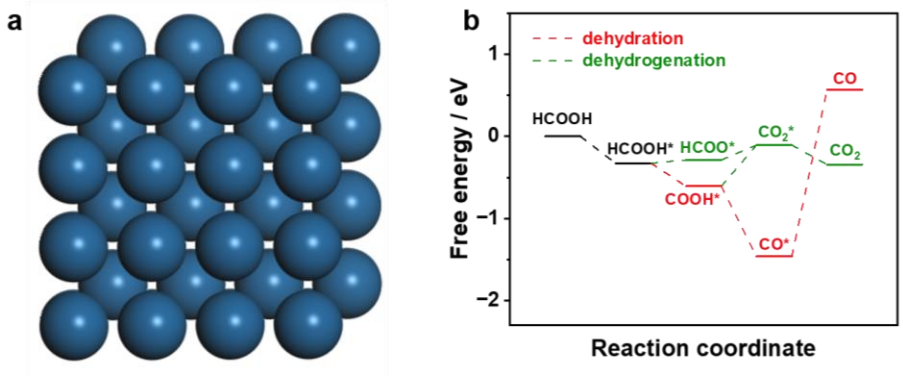

Supplementary Figure 19. (a) Slab model of Pt (100) surface. (b) The corresponding reaction energy diagram of Pt adsorption site.

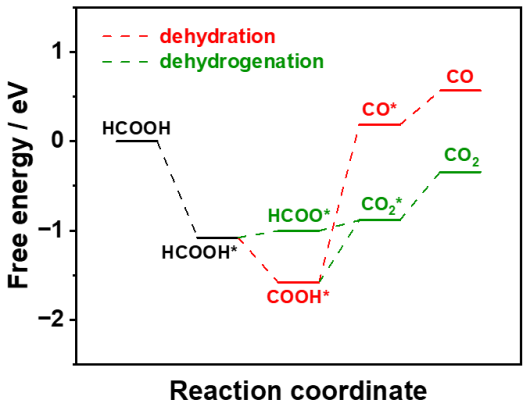

Supplementary Figure 20. The reaction energy diagram of Y adsorption site for Pt (100) surface with single Y site.

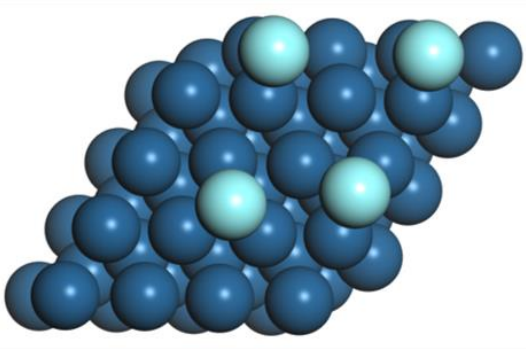

Supplementary Figure 21. Slab model of Pt (111) surface, which failed to be optimized.

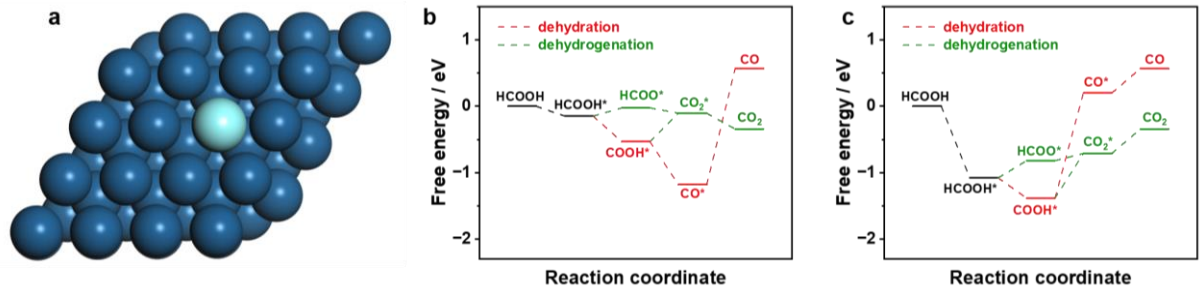

Supplementary Figure 22. (a) Slab model of Pt (111) surface with single Y site. The corresponding reaction energy diagrams of (b) Pt adsorption site and (c) Y adsorption site.

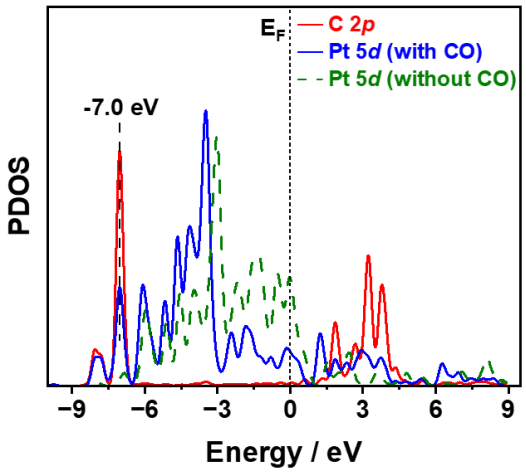

Supplementary Figure 23. PDOS of C 2*p* and Pt 5*d* orbitals in the context of CO adsorption.

Supplementary Table 1. The mass activity comparison between (Y-Pt)-$PtTe_2$ HPNT/C and recently reported Pt-based catalysts for FAOR.

Catalyst	Electrolyte	Mass activity ($A\ mg_{PGM}^{-1}$)	Ref.
(Y-Pt)-$PtTe_2$ HPNT/C	**0.5 M H_2SO_4 + 0.5 M HCOOH**	**6.4**	**This work**
$Pt_{45}Sn_{25}Bi_{30}$	0.5 M H_2SO_4 + 1.0 M HCOOH	4.4	*Adv. Mater.* **2019**, 31, 1903683.
PtCuNi c-NFs	0.5 M H_2SO_4 + 0.25 M HCOOH	0.5	*J. Mater. Chem. A* **2019**, 7, 19280-19289
D-Pt_3Ni-C-600	0.5 M H_2SO_4 + 0.5 M HCOOH	2.8	*J. Energy Chem.* **2019**, 35, 9-16
Pt_3Ag NCs	0.1 M $HClO_4$ + 1.0 M HCOOH	0.2	*Nano Res.* **2019**, 12, 323-329
$PtCu_3$/C	0.5 M H_2SO_4 + 0.25 M HCOOH	0.5	*ACS Appl. Energy Mater.* **2020**, 3, 1010-1016
$Pt_{0.05}Au$/C	0.5 M H_2SO_4 + 0.5 M HCOOH	5.0	*Int. J. Hydrogen Energy* **2020**, 45, 16071-16079
Pt_1Ru_2/MPC 950	0.5 M H_2SO_4 + 1.0 M HCOOH	2.4	*Front. Chem.* **2020**, 8, 367
PtCuNi eb-NFs	0.5 M H_2SO_4 + 0.25 M HCOOH	0.3	*Chem. Mater.* **2020**, 32, 1581-1594
Pd_4Pt_1-CNC	0.1 M $HClO_4$ + 0.1 M HCOOH	2.3	*Electrochim. Acta* **2020**, 354, 136654
$Pt_{20\%}$/Sb	0.1 M $HClO_4$ + 0.1 M HCOOH	0.3	*Research* **2020**, 5487237
0.5%Sn/Pt_3Mn	0.5 M H_2SO_4 + 0.25 M HCOOH	0.1	*J. Catal.* **2021**, 395, 282-292
PtBi@Pd HNPs	0.5 M H_2SO_4 + 1.0 M HCOOH	4.2	*J. Mater. Chem. A* **2021**, 9, 9602-9608
AgPtAu octahedra	0.1 M $HClO_4$ + 0.5 M HCOOH	2.1	*J. Phys. Chem. C* **2021**, 125, 16984-16994
$Cu_{23}Pt_{77}$	0.1 M $HClO_4$ + 0.5 M HCOOH	0.3	*ACS Appl. Nano Mater.* **2021**, 4, 13149-13157
Pt-Bi/Au NPs	0.1 M H_2SO_4 + 1.0 M HCOOH	0.1	*Catalysts* **2021**, 11, 1049
Au@Pt-Pd H-Ss	0.5 M H_2SO_4 + 1.0 M HCOOH	4.4	*Adv. Mater.* **2021**, 33, 2100713
$Au_{90}Pt_{10}$	0.5 M H_2SO_4 + 0.5 M HCOOH	1.9	*ACS Sustainable Chem. Eng.* **2021**, 9, 11062-11069
$Pt_{85}Bi_{15}$ NPs/C	0.1 M $HClO_4$ + 0.1 M HCOOH	1.5	*ACS Appl. Energy Mater.* **2021**, 4, 9190-9197
PtAu/CoNC-3	0.5 M H_2SO_4 + 1.0 M HCOOH	0.9	*Nano Res.* **2022**, 15, 1221-1229
Pd/^{SD}Pt NTs/C	0.5 M H_2SO_4 + 0.5 M HCOOH	2.5	*Chem. Eng. J.* **2022**, 451, 138786
PtBiPbNiCo HEA HPs/C	0.5 M H_2SO_4 + 0.5 M HCOOH	7.1	*Angew. Chem. Int. Ed.* **2023**, 62, e202213783
PtPbBi/PtBi NPs/C	0.5 M H_2SO_4 + 0.5 M HCOOH	7.4	*J. Am. Chem. Soc.* **2023**, 145, 15109-15117
m-PtTe NT/C	0.5 M H_2SO_4 + 0.5 M HCOOH	3.2	*J. Am. Chem. Soc.* **2023**, 145, 15393-15404

Supplementary Table 2. MEA performance comparison between (Y-Pt)-$PtTe_2$ HPNT/C and state-of-the-art Pt-based electrocatalysts as anodic catalysts in DFAFC device from other published works.

Catalyst	Open-circuit voltage in single cell (V)	Anodic Pt loading (mg_{Pt} cm^{-2})	Maximum power density (W g_{Pt}^{-1})	Enhancement factor (vs. commercial Pt/C)	Ref.
(Y-Pt)-$PtTe_2$ HPNT/C	**0.82**	**0.5**	**281.9**	**2.4**	**This work**
PtPb-9-OMCS	0.82	1.2	239.8	1.5	*ACS Nano* **2012**, 6, 6870–6881
Pt-Ni(mqph)	0.80	0.2	166.0	1.9	*J. Appl. Electrochem.* **2016**, 46, 901–905
Dendritic Pt/C	0.58	2.0	21.0	0.9	*J. Appl. Electrochem.* **2017**, 47, 735–745
Bi/Pt NP	0.84	3.0	45.0	1.9	*Electrochim. Acta* **2018**, 273, 307e317
G-cys-Au@Pt	0.83	0.64	198.4	2.2	*Adv. Energy Mater.* **2018**, 8, 1702609
Pt_yPd_x nanoleaf	0.74	2.0	24.6	/	*Ionics* **2018**, 24, 3937–3947
Bi modified Pt/C	0.85	1.2	159.2	2.9	*Appl. Catal. B* **2019**, 253, 187–195
PtCu@NCC	0.75	2.4	50.4	2.3	*Part. Part. Syst. Charact.* **2019**, 36, 1900100
UCS-PtZn iNPs	0.70	1.8	59.4	2.7	*ChemElectroChem* **2019**, 6, 2316
PtCu NW GDE	0.71	2.0	58.2	1.7	*ACS Appl. Mater. Interfaces* **2022**, 14, 11457–11464
PtBiPbNiCo HEA HPs/C	0.70	0.5	642.4	3.7	*Angew. Chem. Int. Ed.* **2023**, 62, e202213783
PtPbBi/PtBi NPs/C	0.83	0.5	323.0	/	*J. Am. Chem. Soc.* **2023**, 145, 15109–15117

Supplementary Table 3. The surface atomic ratios and the valence state analyses for (Y-Pt)-$PtTe_2$ HPNT/C, (Sm-Pt)-$PtTe_2$ HPNT/C, Pt-$PtTe_2$ HPNT/C and commercial Pt/C, as revealed by XPS.

Catalyst	Pt/Te	Pt/Te/RE	Pt^0 (%)	Pt^{2+} (%)	Pt^0/Pt^{2+}	Te^0 (%)	Te^{4+} (%)	Te^0/Te^{4+}
(Y-Pt)-$PtTe_2$ HPNT/C	/	53.2/40.2/6.6	46.1	53.9	0.86	55.3	44.7	1.24
(Sm-Pt)-$PtTe_2$ HPNT/C	/	53.3/40.3/6.4	49.7	50.3	0.99	42.8	57.2	0.75
Pt-$PtTe_2$ HPNT/C	61.2/38.8	/	41.1	58.9	0.70	44.9	55.1	0.81
Commercial Pt/C	/	/	54.1	45.9	1.18	/	/	/